FILE COPY

(4)

Structural Characteristics of Boron-Implanted CdTe

F. W. ADAMS, and J. F. KNUDSEN

AD-A196 215

APPROVED FOR PUBLIC RELEASE;
DISTRIBUTION UNLIMITED

DTIC
ELECTE
JUN 20 1988
S D
H

066

UNCLASSIFIED

SECURITY CLASSIFICATION OF THIS PAGE

REPORT DOCUMENTATION PAGE

1a. REPORT SECURITY CLASSIFICATION: Unclassified

1b. RESTRICTIVE MARKINGS:

2a. SECURITY CLASSIFICATION AUTHORITY:

2b. DECLASSIFICATION / DOWNGRADING SCHEDULE:

3. DISTRIBUTION / AVAILABILITY OF REPORT: Approved for public release; distribution unlimited.

4. PERFORMING ORGANIZATION REPORT NUMBER(S): TR-0086A(2945-07)-4

5. MONITORING ORGANIZATION REPORT NUMBER(S): SD-TR-88-62

6a. NAME OF PERFORMING ORGANIZATION: The Aerospace Corporation Laboratory Operations

6b. OFFICE SYMBOL *(If applicable)*:

7a. NAME OF MONITORING ORGANIZATION: Space Division

6c. ADDRESS *(City, State, and ZIP Code)*: El Segundo, CA 90245

7b. ADDRESS *(City, State, and ZIP Code)*: Los Angeles Air Force Base, Los Angeles, CA 90009-2960

8a. NAME OF FUNDING / SPONSORING ORGANIZATION:

8b. OFFICE SYMBOL *(If applicable)*:

9. PROCUREMENT INSTRUMENT IDENTIFICATION NUMBER: F04701-85-C-0086

8c. ADDRESS *(City, State, and ZIP Code)*:

10. SOURCE OF FUNDING NUMBERS

PROGRAM ELEMENT NO.	PROJECT NO.	TASK NO.	WORK UNIT ACCESSION NO.

11. TITLE *(Include Security Classification)*: Optical and Structural Characterization of Heavily Boron-Implanted CdTe

12. PERSONAL AUTHOR(S): Bowman, R. C. Jr., Alt, R. L., Adams, P. M., and Knudsen, J. F.

13a. TYPE OF REPORT:

13b. TIME COVERED: FROM ______ TO ______

14. DATE OF REPORT *(Year, Month, Day)*: 1988, May 24

15. PAGE COUNT: 26

16. SUPPLEMENTARY NOTATION:

17. COSATI CODES

FIELD	GROUP	SUB-GROUP

18. SUBJECT TERMS *(Continue on reverse if necessary and identify by block number)*: Implant damages, Interstitials, Heavy ions, Photoreflectance

19. ABSTRACT *(Continue on reverse if necessary and identify by block number)*

CdTe single crystals were subjected to multiple-energy boron ion implants with total doses up to 1.5×10^{16} B^{+} ions/cm^2. Various diagnostic techniques were used to assess the structural and electronic properties of these crystals in their as-implanted condition and after anneals under vacuum. The degradation of crystallinity following the boron implants was clearly evident. Annealing temperatures up to 500°C were not effective removing the damage from these heavy dose implants. The chosen boron implant conditions and annealing procedures have not produced substitutional boron donor centers. Excellent correlations were obtained for model calculations of boron projected range and implant damage profiles with the corresponding experimental parameters.

20. DISTRIBUTION / AVAILABILITY OF ABSTRACT: ☒ UNCLASSIFIED/UNLIMITED ☐ SAME AS RPT ☐ DTIC USERS

21. ABSTRACT SECURITY CLASSIFICATION: Unclassified

22a. NAME OF RESPONSIBLE INDIVIDUAL:

22b. TELEPHONE *(Include Area Code)*:

22c. OFFICE SYMBOL:

DD FORM 1473, 84 MAR — 83 APR edition may be used until exhausted. All other editions are obsolete.

SECURITY CLASSIFICATION OF THIS PAGE

UNCLASSIFIED

PREFACE

We wish to thank R. E. Robertson for assistance with the samples, S. N. Witt and K. Kanes for their help with the EPR and Raman measurements, and Dr. F. H. Pollak for his independent Raman study of our samples.

Accession For
NTIS GRA&I
DTIC TAB
Unannounced
Justification
By
Distribution/
Availability Codes
Dist | Avail and/or Special
A-1

CONTENTS

FIGURES

1. INTRODUCTION

While ion implantation has been used to fabricate optoelectronic devices from several II-VI semiconductors, the fundamental processes involved in the creation and fate of various defects remain poorly understood (Ref. 1). There have been numerous instances of contradictory interpretations of defect formation and identification for similar implant and annealing conditions. For example, boron ion implants have been widely used to form n^+-p diode junctions in $Hg_{1-x}Cd_xTe$ for infrared detector applications (Refs. 1,2). However, the extent that the implanted boron becomes electrically active after suitable annealing treatments (Refs. 2,3) is still unresolved. This report describes experimental observations of the structural and electronic properties of CdTe single crystals that have been heavily implanted with boron ions. The techniques include electron paramagnetic resonance (EPR), neutral depth profiling (NDP), double-crystal X-ray diffraction (DCXRD), photoreflectance (PR) spectroscopy, Raman light-scattering, and Rutherford backscattering spectrometry (RBS). In many instances, sequential measurements with several techniques have been performed on the same specimen after an implant or processing treatment. Consequently, variations in crystalline uniformity have been minimized. The objective of these measurements is to compare the distinct information provided by each method in order to develop a comprehensive microscopic assessment of both the implant damage and lattice recovery mechanisms. Partial success towards this goal has been obtained through correlations between the optical properties and various structural characteristics provided by the RBS and DCXRD results. However, detailed evaluations have been elusive due to the complex nature of defect interactions (Refs. 4-6) in CdTe during the implants and anneals. Furthermore, only incomplete recovery of the implant damage was obtained at the highest anneal temperature of 500°C and there was no evidence for the electrical activation of the implanted boron after any treatment.

2. SAMPLE DESCRIPTIONS AND IMPLANT CONDITIONS

Single crystal wafers with (100) and (111) faces were obtained from a master undoped CdTe crystal that had been grown by II-VI Incorporated of Saxonburg, PA. The vendor reported a resistivity of 6.0×10^7 ohm-cm and an etch pit density of 2.4×10^5 cm^{-2} for this crystal. A dilute bromine-methanol etching solution and a polishing pad were used to polish the CdTe wafers prior to the boron ion implants.

Two different, multiple energy boron implant procedures that were used for the CdTe samples are summarized in Table 1. The type A implant deposited $^{11}B^+$ ions to a total dose of 1.0×10^{16} ions/cm^2 while $^{10}B^+$ ions were deposited to a total dose of 1.5×10^{16} ions/cm^2 for the type B implant. In both cases several samples were mounted on silicon substrates with Apiezon black wax and simultaneously implanted with low ion beam currents at room temperature to avoid inadeverent heating effects. The 200°C anneals were performed for one hour in a flowing N_2 gas stream. The implanted CdTe crystals were sealed in evacuated quartz tubes for the nominal 500°C anneals, which were held at this temperature for one hour before an air quench back to room temperature. Although the vacuum anneals probably generated some Cd vacancies, there were no clear indications of any important contributions from these defects to the present results. For example, no significant differences had been observed from DCXRD, EPR, PR, and Raman measurements that were performed before and after 500°C anneals on unimplanted CdTe crystals.

Table 1. Summary of Conditions for Nominal Room Temperature Boron Implants into CdTe Single Crystals

Type Label	Ion Species	Ion Energy (keV)	Ion Dose at Each Energy (10^{15}) (ions/cm^2)	Total Boron Implant Dose (10^{16}) (ions/cm^2)
A	$^{11}B^+$	100	2.5	
		200	2.5	
		300	2.5	1.0
		400	2.5	
B	$^{10}B^+$	50	5.0	1.5
		100	10.0	

3. CHARACTERIZATION METHODS AND RESULTS

3.1 NEUTRON DEPTH PROFILING (NDP)

Projected ion range calculations for the Type A boron-implant energies (i.e., 100, 200, 300, and 400 keV) predict a broad distribution of boron atoms to more than 1000 nm below the crystal surface, whereas, a much narrower and asymmetric boron profile centered near 250 nm is predicted for the type B implant conditions of 50 and 100 keV energies. The NDP technique (Refs. 7, 8) is a non-destructive method to determine the concentration and distribution of the boron-10 isotope (^{10}B) in materials. Figure 1 presents the ^{10}B NDP profiles for (111)-CdTe samples in the as-implanted Type B conditions and after a 499°C anneal. Also included in Fig. 1 is the predicted boron profile for a 50 keV/100 keV double implant generated by the TRIM-86 version of the Monte Carlo-projected range computer code developed by Ziegler et al. (Ref. 9). The NDP measurements yield a boron peak in CdTe near 220 nm for the unannealed type B implant conditions, which is in good agreement with the calculated peak depth, although TRIM predicted a peak ^{10}B content of 5×10^{20} cm^{-3} compared to 4×10^{20} cm^{-3} from the NDP measurement. Furthermore, the NDP ^{10}B profiles are skewed beyond the surface due to an instrumental "pulse pile-up" effect (Ref. 8) that is caused by electrons emitted by the Cd and Te constituents during the neutron irradiations. However, the distortion of the NDP ^{10}B profile is not severe enough to cause all the deviations from the TRIM-calculated curve, and the two distributions are considered to be in reasonable agreement.

The influence of a one hour 499°C anneal on the boron profile in CdTe was also determined by NDP. The ^{10}B profile for the annealed sample is shown in Fig. 1 to be shifted towards the surface, but the shape of the profile remains virtually unchanged. These results imply that about a 25 nm thick surface layer of material was removed during the anneal, but that the implanted boron atoms in Cdte underwent minimal diffusion for these conditions.

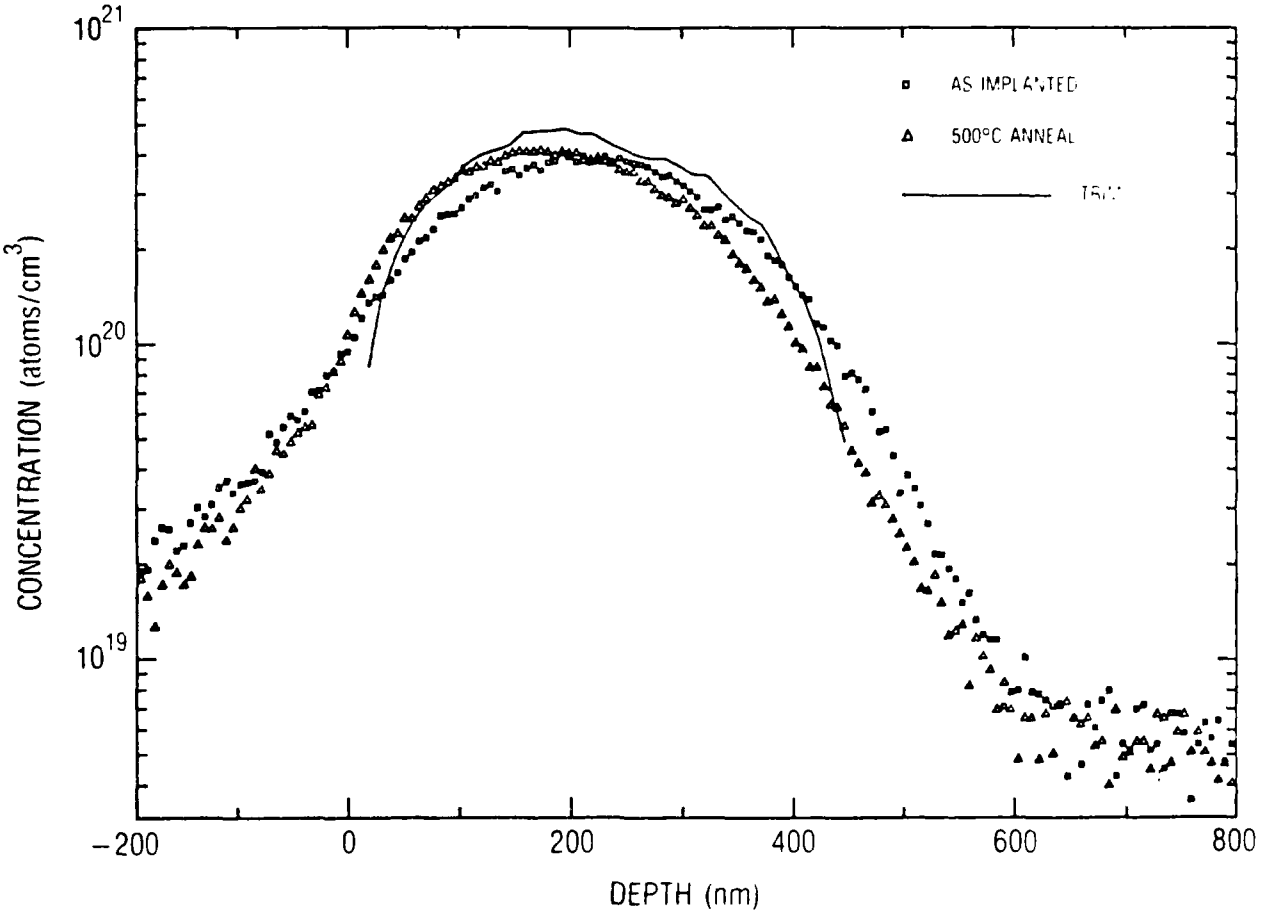

Fig. 1. Boron (^{10}B) Distribution in (111)-CdTe After a 50/100 keV Double Implant and a Post-implant 499°C Vacuum Anneal. The solid curve is the calculated boron profile for as-implanted condition by the method described in the text.

Unfortunately, no CdTe crystals were implanted with ^{10}B ions that correspond to type A conditions (i.e., 100, 200, 300, and 400 keV energies). However, these implants were performed on a $Hg_{0.7}Cd_{0.3}Te$ crystal, and NDP measurements (Ref. 10) confirmed a nearly uniform ^{10}B concentration between the surface and 1000 nm into the crystal. A similar distribution is expected for the Type A $^{11}B^{+}$ implants into the CdTe crystals.

3.2 RUTHERFORD BACKSCATTERING SCATTERING (RBS)

RBS and ion channeling have provided insightful information on ion implantation damage in numerous semiconductors that include $Hg_{1-x}Cd_xTe$ materials (Refs 1-4). For example, Gettings and Stephens (Ref. 4) used RBS to characterize the effects of several heavy ions (e.g., Ar, In, Te, and Bi) on CdTe as well as the reduction of damage under various annealing conditions.

The behavior of CdTe to the boron implants has been studied to analyze the channeling properties of 2 MeV $^{4}He^{+}$ ions. The RBS spectra were obtained with the detector located at 170° relative to the incident He ion beam. Figure 2 compares the RBS spectra for randomly oriented and aligned directions from (111)-CdTe wafers that are unimplanted or subjected to Type B boron implants. The channeled spectra for the unimplanted crystal had a minimum yield (χ_{min}) of 17% below the surface peaks. Thus, this material is of reasonable crystal quality, but it is not as perfect as some other CdTe crystals previously studied (Ref. 4). After the Type B implant, the RBS spectra show that a heavily damaged region has been formed below the surface, which extends to a depth of approximately 450 nm. At the center of the damage region, the χ_{min} value has increased to 83% of the randomly aligned intensity. This result demonstrates that the boron implants did not make the CdTe crystal completely amorphous.

The backscattering yield from the boron implanted CdTe crystals aligned with the He beam usually has two contributions in the analysis beam (Ref. 11). The first is the directly scattered fraction from atoms that are displaced from lattice sites into the crystal channels (i.e., interstitials). The second contribution arises when the analysis beam is

dechanneled by small-angle scattering events with implant-induced damage centers such as dislocations. The approximate number of displaced atoms in boron implanted CdTe was estimated to 2×10^{17} cm^{-2}. This value was obtained from the channeled yield for the as-implanted spectra in Fig. 2. The defect scattering factor was assumed equal to unity [which is valid when all the scattering centers are displaced atoms (Ref. 11)] and the dechanneled fraction was approximated by a straight line that connected the local minimum beneath the Cd surface peak in the RBS spectrum for the aligned unimplanted crystal to the local minimum behind the damaged region for the aligned as-implanted crystal in Fig. 2. The area between this line and the backscattering yield for the aligned as-implanted crystals was used to calculated the approximate number (Ref. 12) of scattering centers (i.e., displaced host atoms). Since the total implanted boron dose for Type B implant condition was 1.5×10^{16} cm^{-2}, the ion channeling result of 2×10^{17} cm^{-2} scattering centers suggests that each ^{10}B ion causes many host atoms to be displaced from their initial lattice sites.

The channeling results in Fig. 2 for the as-implanted and annealed (111)-CdTe crystals clearly show that the one hour 499°C vacuum anneal was unable to remove the damage generated by the Type B boron implants. In fact, only very minor differences are detected in the damage profiles represented by the aligned backscattering yields.

3.3 DOUBLE-CRYSTAL X-RAY DIFFRACTION (DCXRD)

Measurement of X-ray rocking curves (or DCXRD) can determine the crystalline perfection of single-crystal semiconductors (Refs. 13, 14). Furthermore, Speriosu et al. (Ref. 15) have used DCXRD to monitor the damage and strain of ion-implanted GaAs, Si, and Ge. The X-ray rocking curves studies of boron implanted CdTe have been done with Cu $K_{\alpha 1}$ radiation that was initially diffracted with the (400) reflection from a Ge monochromator crystal. The (400) and (333) reflection peaks were obtained from approximately 1 mm^2 areas of the (100) and (111) CdTe samples, respectively. Prior to the boron implants, the present CdTe crystals gave high-quality diffraction peaks (Refs. 13, 14) with full-width, half-maximum linewidths

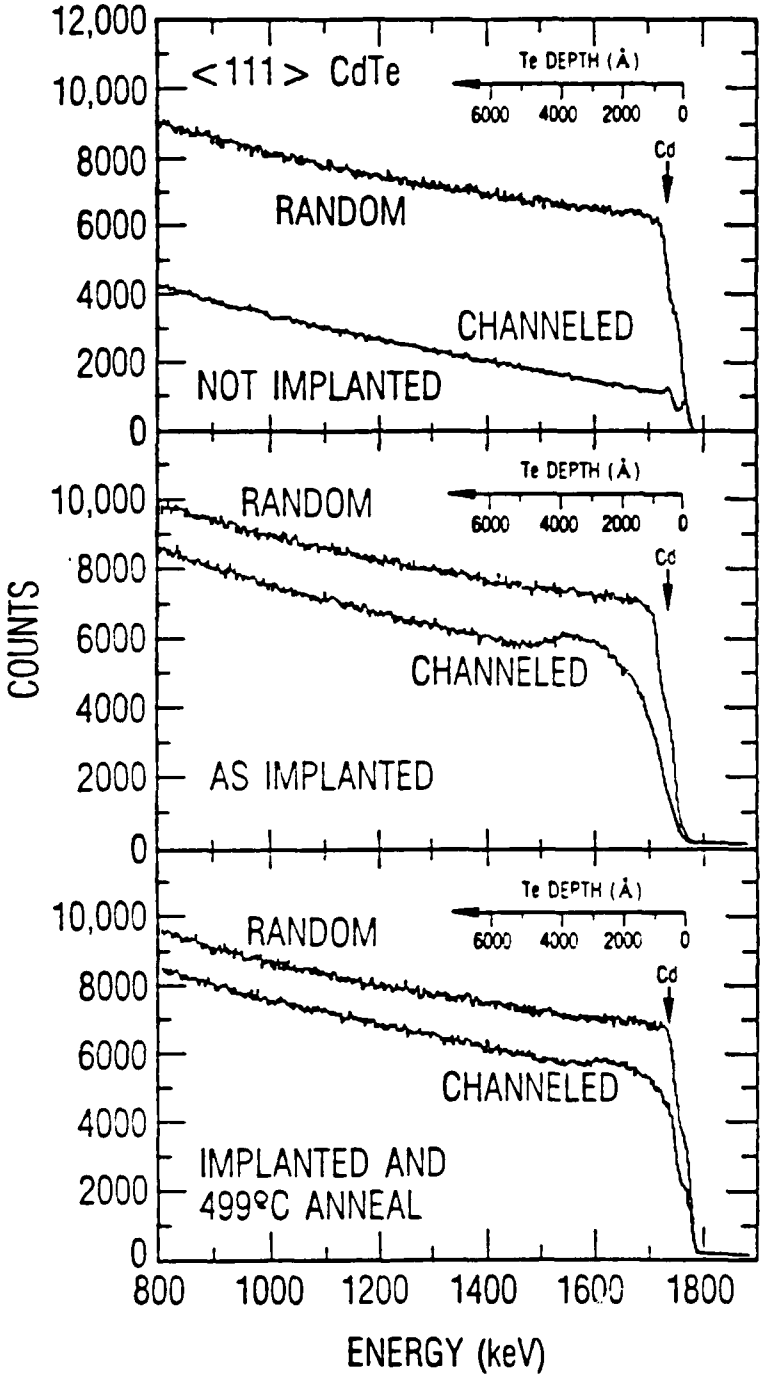

Fig. 2. Rutherford Backscattering Spectra along Random and Channeled Directions from Unimplanted and Type B Boron Implanted (111)-CdTe Crystals

(Γ_{XR}) between 23 and 30 arc-secs. Figure 3 illustrates the effects of a Type A boron implant and subsequent 200°C and 493°C anneals on the rocking-curve peak for (100) CdTe. The boron implant produced a significant reduction in the peak intensity, but only a slightly larger Γ_{XR}. Furthermore, there was no indication of the oscillatory structures caused by implant-induced strains in other semiconductors (Ref. 15). The anneals caused the Γ_{XR} values and peak areas to systematically increase. However, the area of DCXRD peak for the 493°C annealed implanted sample did not recover to the pre-implant value. Similar behavior was observed with the Type B boron implants into (100) and (111) CdTe except that the reduction in peak intensity after the implant was less (i.e., about 15% for Type B versus 40% for Type A) and a correspondingly small recovery was noted following a 499°C anneal. Since the Cu Xrays probe about 4.5 μm into CdTe, these results imply that Type A boron implants cause much deeper damage regions to form than for the Type B implants. This conclusion assumes that little diffracted intensity originates from the damaged region, which is highly disordered but not amorphous, as indicated by the ion channeling studies. The remaining narrow DCXRD peaks arise primarily from deeper-lying undamaged crystal. The nominal 500°C anneals cause a partial recovery of the damaged crystal as the DCXRD peak areas are increased, but an asymmetric broadened with larger Γ_{XR} suggests considerable residual damage is present.

3.4 PHOTOREFLECTANCE (PR) SPECTROSCOPY

Photoreflectance is a variation of modulation spectroscopy that can provide sharp derivative-like spectra at energies associated with optical transitions between critical point energies in semiconductor band structures. Vazquez-Lopex et al. (Ref. 16) have used PR to determine the quality of polycrystalline CdTe thin films in which the phenomenological lineshape parameters (Γ) from the Aspnes function (Ref. 17) were fitted to their band-gap (i.e., E_o) PR spectra. Brown et al. (Ref. 18) used the electrolyte electroreflectance (EER) version of modulation spectroscopy to examine ion-implant damage in GaAs as well as subsequent recovery of crystalline quality with anneals. They showed that implants caused extensive

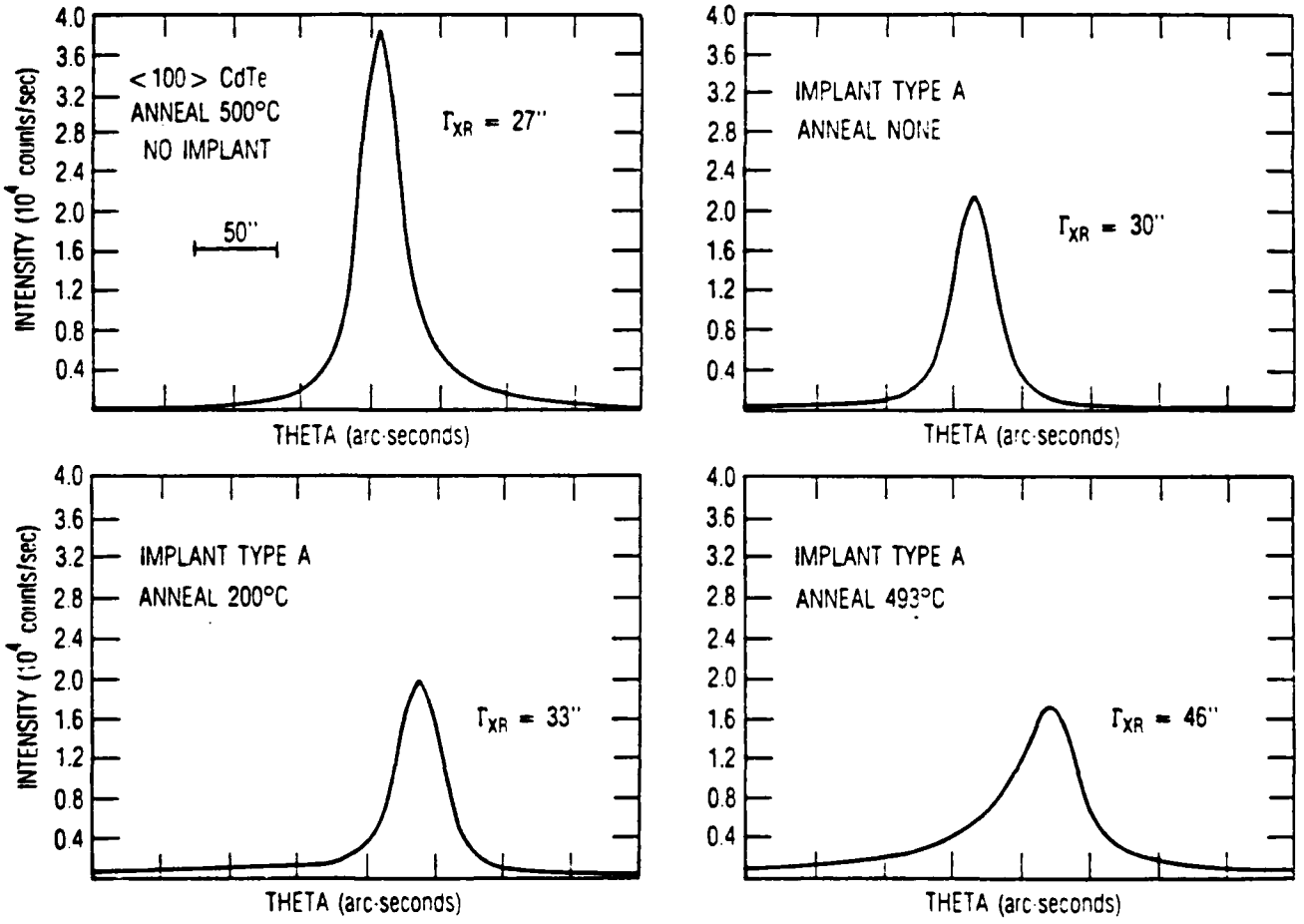

Fig. 3. Comparisons of (400)-Reflections From Double-crystal X-ray Diffraction on Unimplanted and Type A boron Implanted (100)-CdTe

broadening of the E_0 and E_1 transitions. These peaks would become sharper upon annealing treatments that restored crystallinity.

Room temperature PR measurements have been performed on numerous CdTe crystals to assess crystalline quality and the effects of the boron implants. Representative PR spectra for the same CdTe samples given in Fig. 3 are presented in Fig. 4. A 1 mW HeNe laser was used for the pump beam and the probe beam light from a 100 W quartz halogen lamp was passed through an Instruments SA, Inc. model HR-320 monochromator for detection by a Si-photodiode (Ref. 19). The PR spectrum in Fig. 4A for a freshly polished (100) CdTe sample is well represented by a third-derivative lineshape (Ref. 17) with Γ= 17 meV. The remaining PR spectra in Fig. 2 illustrate that a Type A boron implant yields substantial broadening of the E_0 transitions, which can be partially reversed by subsequent anneals. Nevertheless, Γ = 33 meV after the 493°C anneal of the type A implant, which is about 50-100% larger than the linewidth parameters for unimplanted CdTe crystals (Refs. 16,19). The PR spectra for the Type B implants were weaker and broader than the spectrum in Fig. 4B and the 500°C anneals were even less effective in regenerating sharp PR spectra. Another interesting aspect of the PR spectra in Fig. 4 are the small positive shifts of about 15 meV in the E_0 positions for the annealed-implanted samples, compared to the band gaps for the initial CdTe crystals. Brown et al. (Ref. 18) have attributed similar shifts in the E_1 transitions for their annealed-implanted GaAs samples to impurity modifications of the band structure. Whether this mechanism is applicable to the implanted CdTe samples is currently unclear, although boron could serve as a donor center if these atoms occupy the Cd lattice sites.

3.5 RAMAN SPECTROSCOPY (RS)

Raman light scattering measurements of the phonon modes have been very successful for microscopic evaluations of ion-implant damage in silicon (Ref. 20) and III-V semiconductors (Ref. 21). The intensities and linewidths of the longitudinal (LO) and transverse (TO) optic phonons are quite sensitive to crystalline quality. The detection of phonon frequencies in CdTe by RS can be difficult due to their proximity to the laser excitation line and stray light

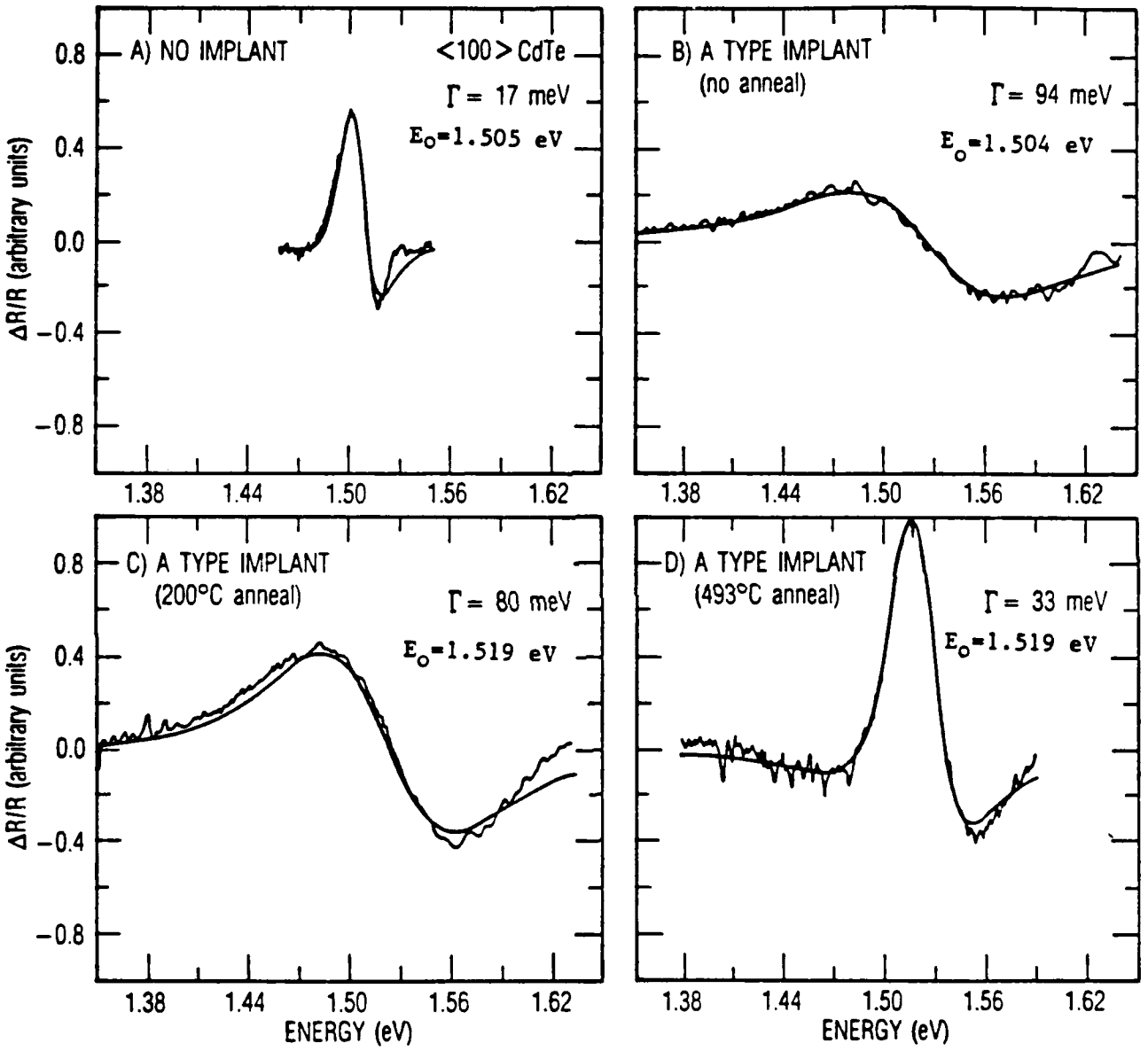

Fig. 4. Photoreflectance Spectra in Band-gap Region for the (100)-CdTe Samples From Fig. 3

scattering from irregular crystal surfaces (Ref. 22). The Raman measurements of LO phonons from (100) CdTe surfaces were made with considerable effort in the conventional backscattering geometry. The room temperature samples were illuminated nominally with 200 mW of filtered light from the 488 nm line of an Argon-ion laser. The cross-polarized scattered light was analyzed with a Spex double monochromator and cooled photomultiplier tube. The cross-polarized RS spectra for Type B implanted and implanted-anneal (100) CdTe crystals are compared in Fig. 5. The very weak peak at 167 cm^{-1} from the as-implanted samples corresponds to the selection rule allowed LO peak (Ref. 22) for this polarization configuration. The 499°C anneal causes the intensity of this peak to increase substantially. Independent RS measurements on these same samples by Prof. F. H. Pollak have confirmed the results in Fig. 5. Since RS can probe CdTe to depths less than 100 nm below the crystal surface, the spectra in Fig. 5 implies that 500°C anneals can lead to improvement (Refs. 20, 21) in the crystallinity in the near surface region of CdTe. This observation does not contradict the absence of substantial lattice recovery from Type B implants that was indicated by the RBS, DCXRD, and PR experiments. These latter techniques usually sample much deeper regions into the crystal (i.e., their total depth ranges can be greater than 1000 nm). Furthermore, the maximum damage from the boron implants should be deeper than 100 nm, which are in regions that can not be investigated by the available RS laser-line excitation source.

3.6 ELECTRON PARAMAGNETIC RESONANCE (EPR)

EPR spectroscopy is another powerful method to characterize defects and impurities in semiconductors and is the final technique that has been applied to the boron-implanted CdTe crystals. The EPR experiments were performed with a Varian E-line spectrometer and an X-band microwave cavity. An Air-Products Heli-Tran gas transfer Dewar was used to cool samples to temperatures between 5 K and 20 K. In order to detect photon-sensitive paramagnetic defects, samples could be in-situ illuminated with a 250 watt He-Xe lamp. Prior to the boron implants, none of the present CdTe crystals produced any EPR signals (Ref. 23). After both Type A and type B boron implants, a narrow (i.e., peak-

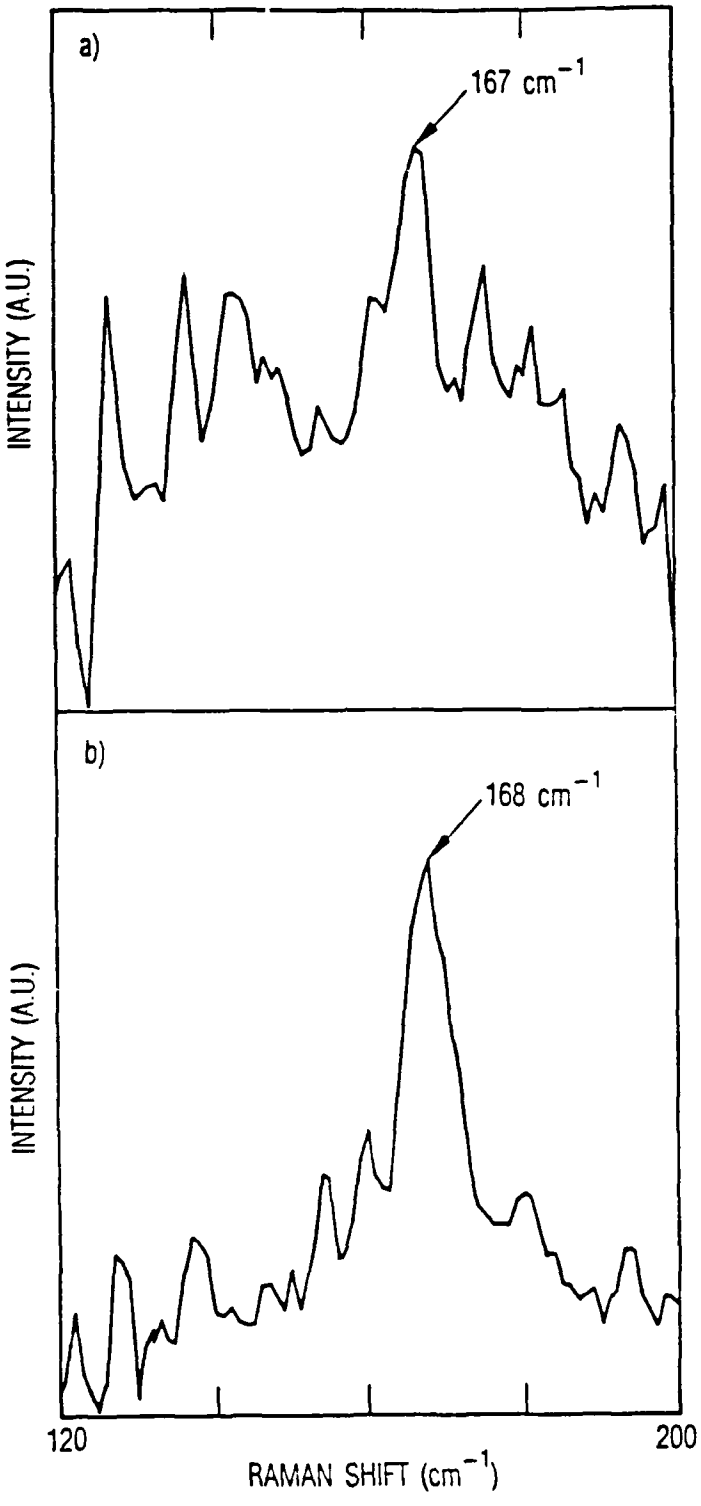

Fig. 5. Raman Spectra from Type B Boron-Implanted (100)-CdTe Crystals That Were Obtained by Method Described in the Text. The arrows denote the longitudinal optic (LO) phonon positions.

to-peak separation about 5 gauss) isotopic peak with a g-factor of 2.003 was observed (Ref. 23). The intensity of this EPR signal was much greater for the Type B implants. The nominally 500°C anneals could greatly reduce its magnitude, but the changes were not very reproducible. While it is very tempting to attribute this EPR peak to a defect in CdTe, very similar signals at g = 2.0028 (2) have been associated (Refs. 24, 25) with carbon dangling bonds in contamination films on semiconductor surfaces. Hence, it is very possible that a similar source introduced during the implantation may be responsible for the g = 2.003 EPR peaks from the present CdTe samples. Additional studies are in progress to clarify whether contamination has actually occurred. However, conspicously absent from the EPR spectra, for annealed as well as unannealed boron implanted CdTe, were the characteristic signals at g = 1.65 to g = 1.70 from paramagnetic shallow donor centers as were reported (Ref. 26) for Cl, In, and Al doped CdTe. If the implanted boron atoms formed these shallow donor states, EPR signals similar to those described by Saminadayer, et al. (Ref. 26) should have been detected. On the other hand, if the boron atoms formed deep donor states upon electrical activation, EPR signals near g = 2.0 with pronounced boron hyperfine structures are anticipated (Ref. 23). Since neither type of EPR spectrum was observed under dark or illuminated conditions from any boron implanted CdTe sample, the present annealing procedures apparently cannot substitutionally activate the boron atoms.

4. DISCUSSION AND CONCLUSIONS

The present boron implants have been found to alter various structural and optical properties of CdTe. The depth and extent of these changes are correlated with both the dose and ion energy of the boron species. Figure 6 compares the displaced atom concentration profile obtained by an analysis of the RBS - channeling results for Type B implanted (111)-CdTe with a TRIM calculation of the profile for damage energy that produces target atom displacements. The agreement is quite satisfactory as both curves predict maximum damage between 100-150 nm, which is somewhat towards the surface from the peak of the deposited boron atoms also shown in Fig. 6. As indicated, most of the damage from the 50/100 keV boron implants vanishes within 500 nm of the surface. While the CdTe lattice is greatly disordered by these implants, the ion channeling results in Fig. 2 clearly indicate this region has not become amorphous. Gettings and Stephens (Ref. 4) had previously found that implants up to doses of 5×10^{16} cm^{-2} also could not produce amorphous regions. They suggested that the ionic character of CdTe and enhanced vacancy mobility prohibited complete disorder of the CdTe lattice. The apparent absence of crystalline strain (as reflected in the X-ray rocking curves) in any of the boron implanted CdTe samples was unexpected in light of the behavior of other semiconductors (Ref. 15) to ion implants. The occurrence of extensive crystal disorder without either lattice strain or amorphicity is an unusual situation. The microscopic processes responsible for this behavior are currently unknown and are worthy of further study.

The available results consistently indicate that the present boron implants as well as thermal anneals to 500°C do not produce electrically-activated boron atoms on a crystalline CdTe lattice. While recent photoluminescence measurements (Ref. 6) implied essentially complete elimination of boron implant damage from CdTe after rapid thermal anneals to 500°C, the total boron dose was only 2.35×10^{13} ions/cm^2 for these samples. Perhaps the approximately 400 larger flux in the present Type A and B boron implants generated damage defects that are much more stable. However, the

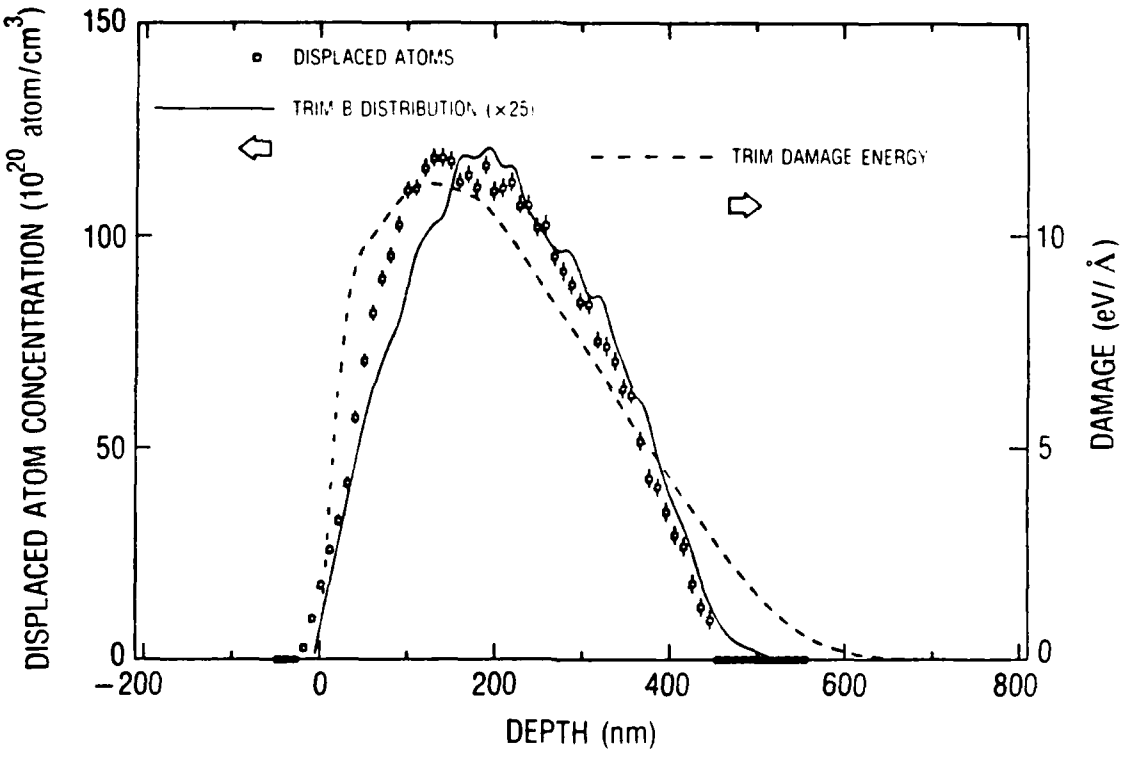

Fig. 6. Comparison of the Distribution of Displaced Atoms from the Channeled RBS Spectrum for Type B Boron Implanted (111)-Cdte and Calculated Boron Profile and Damage Energy Distribution Obtained by the TRIM Simulation Model.

photoluminescence data also indicated that the implanted boron was not behaving as a substitutional donor under these annealing conditions. This latter observation is in complete accord with the present results. In order to determine whether vacancies produced during the anneals have influenced the removal of implant damage or boron activation, future studies will also include anneals under the vapor from Cd metal sealed in the evacuated tubes. These results will be reported elsewhere.

REFERENCES

1. T. W. Sigmon, Nucl. Instrum. Methods B 7/8, 402 (1985).

2. G. L. Destefanis, Nucl. Instrum. Methods 209/210, 567 (1983).

3. T. M. Kao and T. W. Sigmon, Appl. Phys. Lett. 49, 464 (1986).

4. M. Gettings and K. G. Stephens, Radiation Effects 22, 53 (1974).

5. R. Kalish, M. Deicher, and G. Schatz, J. Appl. Phys. 53, 4793 (1982).

6. K. M. James, J. L. Merz, and C. E. Jones, J. Appl. Phys. 60, 3699 (1986).

7. R. G. Downing, R. F. Fleming, J. K. Lang, and D. H. Vincent, Nucl. Instrum. Meth. 218, 47 (1983).

8. R. C. Bowman, Jr., R. E. Robertson, J. F. Knudsen, and R. G. Downing, "Infrared Detectors, Sensors, and Focal Plane Arrays" - SPIE Proceedings Vol. 686, Ed. H. Nakamura (Soc. Photo. Instrum. Eng., Bellingham, WA, 1986) 18.

9. J. F. Ziegler, J. P. Biersack, and U. Littmark, The Stopping and Range of Ions in Solids Pergamon, New York, (1985).

10. R. C. Bowman, Jr., J. F. Knudsen, and R. G. Downing, Trans. Am. Nucl. Soc. 55, 212 (1987).

11. L. C. Feldman, J. W. Mayer, and S. T. Picraux, Materials Analysis by Ion Channeling Academic, New York, 1982.

12. F. H. Eisen, Channeling, Ed. D. V. Morgan, Wiley, New York, 415, (1973). 415).

13. J. H. Dinan and S. B. Qadri, Thin Solid Films 131, 267 (1985).

14. R. F. C. Farrow, J. Vac. Sci. Technol. A3, 60 (1985).

15. V. S. Speriosu, et al. Appl. Phys. Lett. 40, 604 (1982).

16. C. Vazquez-lopez, et al. J. Appl. Phys. 58, 2066 (1985).

17. D. E. Aspnes, Surf. Sci. 37, 418 (1973).

18. R. L. Brown, et al. J. Appl. Phys. 52, 2950 (1981).

19. R. C. Bowman, Jr., R. L. Alt, and K. W. Brown, Proc. Soc. Photo. Instrum. Eng. 794, 96 (1987).

20. K. P. Jain, et al. Phys. Rev B . 32, 6688 (1985).

21. C. S. Rama Rao, et al. J. Appl. Phys. 54, 1808 (1983).

22. P. M. Amirtharaj and F. H. Pollak, Appl. Phys. Lett. 45, 789 (1984).

23. R. C. Bowman, Jr., E. L. Venturini, and S. N. Witt, J. Vac. Sci. Technol. A 5, 3171 (1987).

24. D. J. Miller and D. Haneman, Surf. Sci. 24, 639 (1971).

25. W. E. Carlos, J. Non-Cryst. Solids 66, 157 (1984).

26. K. Saminadayar, D. Galland, and E. Molva, Solid State Commun. 49, 627 (1984).